
Theses and Dissertations

Student Publications

Spring 4-26-2022

Synthesis, Characterization and Activity of Palladium Catalysts on the Dual Support of Cerium and Aluminum Oxides

Jihyeon Park

Follow this and additional works at: https://csuepress.columbusstate.edu/theses_dissertations

 Part of the [Chemistry Commons](#)

COLUMBUS STATE UNIVERSITY

**Synthesis, Characterization and Activity of Palladium Catalysts on the Dual Support of
Cerium and Aluminum Oxides**

A THESIS SUBMITTED TO
THE COLLEGE OF LETTERS AND SCIENCES
IN THE PARTIAL FULFILLMENT OF
THE REQUIREMENTS FOR THE DEGREE OF

MASTER OF SCIENCE

DEPARTMENT OF CHEMISTRY

BY

JIHYEON PARK

COLUMBUS, GEORGIA

2022

Copyright © 2022 Jihyeon Park

All rights reserved.

**Synthesis, Characterization and Activity of Palladium Catalysts on the Dual
Support of Cerium and Aluminum Oxides**

By

Jihyeon Park

Committee Chair:

Dr. Anil C. Banerjee

Committee Members:

Dr. Zewdu Gebeyehu
Dr. Daniel Wade Holley

SUMMARY

The effects of sequence of impregnation (Pd on cerium oxides -alumina and cerium oxides on Pd-alumina) and calcination temperature (500 °C and 850 °C) on the catalytic oxidation of methane under lean conditions were investigated. The catalysts were prepared by a combination of impregnation, slurry and vortexing methods. The catalysts had 4.7 wt.% Pd and 10.7 wt.% Ce based on inductively coupled plasma optical emission spectrometry (ICP-OES) analysis. The catalysts were characterized by pulse chemisorption, temperature programmed reduction (TPD), scanning transmission electron microscopy (STEM), and X-ray photoelectron spectroscopy (XPS). The activity of the catalysts for methane combustion was measured in a fixed-bed flow reactor by flowing a gas mix (0.98 vol % methane, 4.01 vol % and balance nitrogen) through a catalytic bed. The temperature of the catalytic bed was controlled by a temperature -controlled tube furnace. The % methane in the effluent gas mix was measured by a gas chromatograph fitted with a flame ionization detector and a 'Carbon Plot' column. Palladium was present as PdO and PdO_x (x>2+) and cerium as CeO_x (+3 and +4 oxidation states) as per XPS analysis. The activity of the Pd/cerium oxides-alumina500C catalyst was higher than the cerium oxides/Pd-alumina500C catalyst at 250-500 °C. Similar trends in the activity were seen for the two catalysts calcined at 850 °C. Higher dispersion and lower particle size, and the presence of small Pd particles on alumina accounted for the higher catalytic activities of the Pd/cerium oxides-alumina500C and 850C catalysts. The lower activities of cerium oxides/Pd-alumina500C and 850C were primarily due to the embedment of Pd onto ceria due to strong PdO-CeO_x interactions. This research implies that the sequence of impregnation and calcination temperature could alter catalytic properties and activity for methane combustion through PdO/PdO_x -support interactions.

INDEX WORDS: Impregnation sequence, catalyst preparation methods, methane combustion, characterization, metal-support interactions

To
My Family and Peter

Thank you for always being a wonderful family and supporting my studies.

You are the one who made me now!

ACKNOWLEDGEMENTS

I would like to thank my mentor, Dr. Anil Banerjee, Professor of Chemistry at Columbus State University, for guidance and supervision of my graduate thesis research and always encouraging me. I also thank Dr. Gebeyehu and Dr. Holley, Professors of Chemistry at Columbus State University for serving on my thesis committee.

Thanks to Laura Proano Gonzalez, PhD student at the Department of Chemical and Biomedical Engineering, Georgia Institute of Technology for doing the characterization experiments (Pulse chemisorption, Temperature programmed reduction, X-ray photoelectron spectroscopy and Scanning Transmission electron microscopy).

Thanks to Dr. Jackson, Chair of the Chemistry Department at Columbus State University, for encouraging me not to give up on my dreams and not to lose a cheerful outlook.

Thanks to the Student Research and Creative Endeavors (SRACE) grant for awarding research fundings.

TABLE OF CONTENTS

ACKNOWLEDGEMENTS	V
LIST OF TABLES	VIII
LIST OF FIGURES	IX
I. INTRODUCTION	1
A. BACKGROUND INFORMATION	1
B. REVIEW OF LITERATURE	3
C. OBJECTIVES OF THIS STUDY	5
II. METHODS	6
A. CATALYSTS SYNTHESIS	6
i. Pd/Cerium oxide-alumina catalyst calcined at 500 °C	7
ii. Pd/Cerium oxide-alumina catalyst calcined at 850 °C	8
iii. Cerium oxide/Pd-alumina catalyst calcined at 500°C	8
iv. Cerium oxide/Pd-alumina catalyst calcined at 850°C	8
B. CATALYTIC ACTIVITY	9
C. CHARACTERIZATION	11
i. Inductively Coupled Plasma Optical Emission Spectrometry (ICP-OES)	11
ii. Pulse Chemisorption	11
iii. Temperature-Programmed Reduction (TPR)	12
iv. X-Ray Photoelectron Spectroscopy (XPS)	12
v. High-Angle Annular Dark-Field Scanning Transmission Electron Microscopy (HAADF-STEM)	13

III. RESULTS AND DISCUSSION	13
A. ACTIVITY OF THE CATALYSTS.....	13
i.i. Activation energy.....	17
i.ii. Stability test.....	18
B. CHARACTERIZATION	19
ii.i. Inductively Coupled Plasma Optical Emission Spectrometry (ICP-OES).....	19
ii.ii. Pulse Chemisorption.....	20
ii.iii. Hydrogen-Temperature Programmed Reduction (H ₂ -TPR).....	21
ii.iv. X-Ray Photoelectron Spectroscopy (XPS).....	22
ii.v. High-Angle Annular Dark-Field Scanning Transmission Electron Microscopy (HAADF-STEM) and Scanning Electron Microscopy (SEM).....	23
IV. CONCLUSION.....	25
V. BIBLIOGRAPHY	27

LIST OF TABLES

Table 1. Inventory and nomenclature of Pd catalysts	6
Table 2. Activity data on methane combustion at 500 °C and 850 °C with fresh catalysts	13
Table 3. Detailed Activity-Temperature data	15
Table 4. Activity data of cerium-aluminum oxides dual support calcined at 850 °C	16
Table 5. Activation energy	17
Table 6. Stability test on four catalysts	19
Table 7. ICP-OES analysis	20
Table 8. Properties of catalysts	20
Table 9. XPS data	23

LIST OF FIGURES

Figure 1. Greenhouse Gas emissions and Methane emission sources	2
Figure 2. Catalytic converters (Source: AA1Car.com).....	2
Figure 3. Catalyst synthesis apparatus	7
Figure 4. Catalyst bed in reactor	9
Figure 5. Catalytic reactor unit	10
Figure 6. Methane conversion at different temperatures	16
Figure 7. Activation energy for methane combustion with the four catalysts	18
Figure 8. Hydrogen-TPR	22
Figure 9. HAADF-STEM of four catalysts.....	Error! Bookmark not defined.

I. Introduction

A. Background information

Methane is one of the greenhouse gases that affects climate change and global warming. Carbon dioxide, methane, nitrous oxide, fluorinated gases are greenhouse gases. These greenhouse gases contribute to the depletion of the ozone layer above the earth. Even though methane is the second worst greenhouse gas, in the near-term methane has over 80 times the warming effect of carbon dioxide.¹ Also, methane has a shorter lifetime in the atmosphere than carbon dioxide, but methane traps the radiation more and has 25 times greater impact on climate changes.² Therefore, reduction of methane gas emissions is especially important. There are various sources contributing to methane accumulation in the atmosphere. The data given in Figure 1 (Source: Environmental Protection Agency, EPA) shows that about 57 percent of total methane emission comes from natural and petroleum and fermentation industries, and the rest from other human activities. According to the EPA, the oil and gas industry emits eight million metric tons of methane a year.³

Another major issue is the air pollution caused by emissions of methane gas from transport vehicles using compressed natural gas (methane) and diesel fuels. Catalytic converter is a device for vehicles to convert methane and other toxic gases (carbon monoxide, nitrogen oxides) to less harmful gases like carbon dioxide. A catalytic converter has two types of catalysts at work, a reduction catalyst, and an oxidation catalyst. Both types consist of a ceramic honeycomb structure coated with metals (Platinum, rhodium, or palladium) and support (aluminum oxide, cerium oxide) to convert methane, carbon monoxide, and nitrogen oxides to carbon dioxide, water, and nitrogen. A detailed description of a catalytic converter is given in Figure 2.

A catalytic converter works very well at an elevated temperature of 800-900 °C. The heat produced in automobile engines is transferred to the catalytic converters to keep this temperature range.

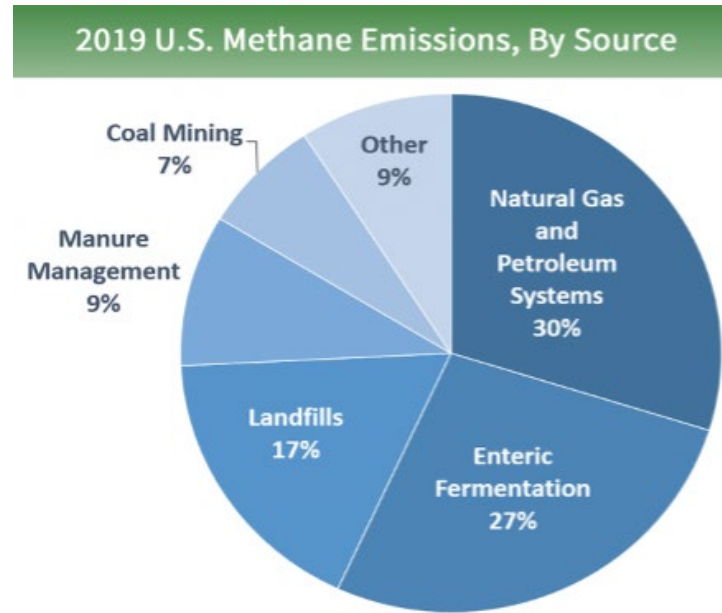


Figure 1. Greenhouse Gas emissions and Methane emission sources

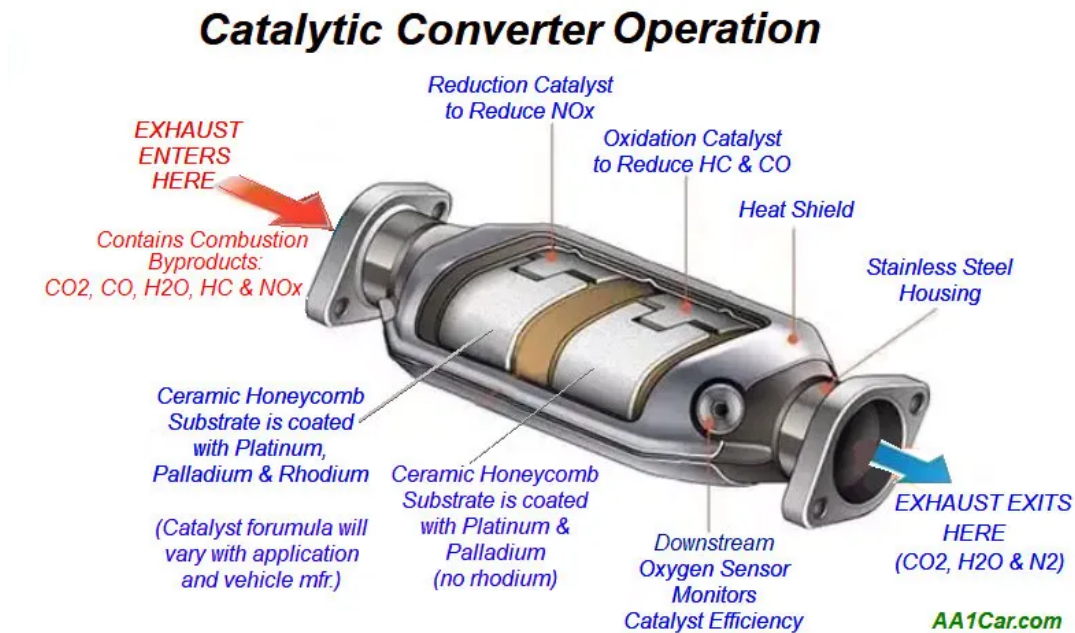


Figure 2. Catalytic converters (Source: AA1Car.com)

However, modern fuel-efficient automobile engines produce less heat for thermal efficiency. This in turn, requires the catalytic converters to work at a lower temperature range of 400-500 °C or less. However, current catalytic converters do not work efficiently at lower temperatures. This results in the emission of unconverted methane and other toxic gases from the tail pipes particularly during wintry weather and ‘Cold Start’. The catalytic combustion of methane has generated tremendous interest in developing environmental catalysts for pollution control caused by automobiles and gas-powered energy generation systems. Additionally, development of catalysts for low-temperature applications has been a challenging issue due to the highly stable carbon-hydrogen bond in the nonpolar CH₄ molecule.³

B. Review of Literature

A review of literature on catalytic oxidation methane is summarized below. Two recent reviews^{4,5} summarized the recent advances made in the catalytic combustion of methane. Methane combustion by palladium catalysts on different supports including alumina⁶⁻⁸, ceria^{9,10} and ceria-alumina have been reported¹¹⁻¹⁵. However, this thesis is focused on palladium metal impregnated on the dual support of cerium oxides (CeO_x) and aluminum oxide (Al₂O₃) for the catalytic combustion of methane under lean conditions (excess air). Hence, this literature survey is primarily on platinum group transition metals on the dual support of CeO_x/Al₂O₃.

Colussi et al¹⁶ studied the catalytic activity of Pd-based catalysts at elevated temperature supported on rare earths oxides and reported that the Pd particles could reoxidize at higher temperature in contact with CeO₂ and improve the catalytic activity.

Cargnello et al¹¹ synthesized Pd on CeO₂/H-Al₂O₃ catalysts by supramolecular approach; Pd as the core and ceria as the shell were preorganized and deposited into a modified hydrophobic alumina. In this case, the Pd cores being isolated led to improved metal-support

interactions and complete conversion of methane below 400 °C and with superior thermal stability under specific condition.

Li et al¹² prepared a moisture-treated Pd/CeO₂/Al₂O₃ core-shell catalyst by mixing desired amount of Al₂O₃ with the Pd/CeO₂ suspension. The catalytic activity showed 90% conversion of CO, hydrocarbons, and NO over the Pd/ CeO₂-Al₂O₃ catalyst at 220 °C, 230 °C, and 220 °C, respectively. Transmission electron microscopy images showed that Pd/CeO₂ nanoparticles had a large amount of PdO₂ on the Pd and CeO₂ interface. Fourier- transform infrared spectra (FTIR) showed the presence of *OOH and *NO₂ intermediate groups and these contributed to higher catalytic activities.

Rodrigues et al¹³ developed Ni and Pd catalysts with Al₂O₃ and CeO₂/Al₂O₃ by impregnation method. The catalytic activity was evaluated using temperature-programmed surface reaction (TPSR) tests over 24 h on stream. The catalysts were characterized by standard characterization techniques. The results showed that the mechanism of partial oxidation of methane was directly connected to the metals, and Pd/Al₂O₃, Pd/CeO₂/Al₂O₃ catalysts had better CH₄ conversion. The catalysts were more resistant to deactivation on the dual support CeO₂/Al₂O₃. The higher oxygen exchange ability of CeO₂ as a support makes the metal surface free of carbon, which promotes better activity.

Ramirez et al¹⁴ synthesized Pd/CeO₂-Al₂O₃ catalysts by sol-gel method with the dual support impregnated onto a palladium nitrate solution in water. Ceria loadings (2, 5, 10, 15, and 50 wt%) were used. The catalyst with a high ceria loading had a reduced surface area and lowest ceria loading in the palladium catalyst gave complete oxidation of methane at 425 °C.

Sun et al¹⁵ investigated the effect of loading sequence in Pd/Ce/Al catalysts on the conversion of lower hydrocarbons. The two catalysts showed a significant difference in both

dispersion and particle sizes. The lower dispersion in the PdO/CeO₂/Al₂O₃ catalyst was due to the PdO particles being fixed on the ceria support by strong Pd-O-Ce bonds.

Liu et al.¹⁷ synthesized the PdO/CeO₂-Al₂O₃ by impregnation of cerium nitrate hexahydrate to γ -Al₂O₃ followed by addition of PdCl₂ under an ultrasonic condition. H₂-temperature programmed reduction and O₂-temperature programmed desorption was used for characterizing the reaction properties on the catalyst surface. The catalyst PdO/CeO₂-Al₂O₃ with rapid activation showed higher activity of methane combustion due to uniformly distributed PdO species on the support surface.

Yang et al.¹⁸ developed a Pd-CeO₂CAS_s/Al₂O₃ catalyst by a novel approach involving synthesis of Pd-CeO₂ colloidal assembled spheres in one-pot fashion. CeO₂ nanocrystals surrounded the Pd clusters and enhanced interface area of Pd/ceria. Pd-CeO₂CAS_s/Al₂O₃ catalyst showed better catalytic activity and stability than a Pd/CeO₂ catalyst. The presence of Pd-O-Ce and surface-active oxygen species could contribute toward catalytic activity.

Fertal et al.¹⁹ did a preliminary study on the effects of impregnation sequence on the catalytic activities of Pd/ceria-alumina catalysts. The research group reported a better catalytic activity for methane oxidation by the Pd/ceria-alumina catalyst compared to the ceria/Pd-alumina catalyst. However, the study had limitations since the reactions were not conducted under the steady state and the catalysts were not characterized completely.

The review of the research literature shows a lack of detailed investigation on the catalytic oxidation of methane by Pd/ceria-alumina and ceria/Pd-alumina catalysts including the effects of the sequence of impregnation, calcination temperature, and metal-support interactions.

C. Objectives of this study

The specific objectives of this research were to investigate:

1. The effect of the sequence of impregnation of Pd and cerium oxides on Pd/cerium oxides-aluminum oxide catalysts on the catalytic oxidation of methane.
2. The correlation between activity, dispersion, and particle size of the catalysts.
3. The correlation between activity, active phases, and metal-support interactions.

II. METHODS

A. Catalysts Synthesis

An inventory of the synthesized catalysts is given in Table 1.

Table 1. Catalyst nomenclature and inventory

Pd/cerium oxides-alumina500C: Pd/cerium oxides-alumina calcined at 500 °C
Pd/cerium oxides-alumina850C: Pd/cerium oxides-alumina calcined at 850 °C
Cerium oxides/Pd-alumina500C: Cerium oxides/Pd-alumina calcined at 500 °C
Cerium oxides/Pd-alumina850C: Cerium oxides/Pd-alumina calcined at 850 °C
Cerium oxides/alumina500C: Cerium oxides/ alumina calcined at 500 °C
Cerium oxides/alumina850C: Cerium oxides/ alumina calcined at 850 °C

The catalysts were synthesized using the apparatus shown in Figure 3. The apparatus consists of a syringe pump and a vertexing unit. The syringe pump delivers the precursor solution from the syringe to the vertexing unit. The catalysts were synthesized by a combination of impregnation, slurry and vortexing methods.²²



Figure 3. Catalyst synthesis apparatus

i. Pd/Cerium oxide-alumina catalyst calcined at 500 °C

An aqueous solution was made by dissolving 0.386 g palladium nitrate hydrate (Aldrich, USA) in 1.5 mL of distilled water. The 3.00 g solid cerium oxide-alumina dual support calcined at 500 °C into the vortex tube and adding 5.0 mL of distilled water to make slurry. An aqueous solution of palladium nitrate hydrate was added in 20 microliter increments to the aqueous solution of the dual support as it was being vortexed at speed 3 for 3 hrs. The slurry was dried in an air oven at 110°C for 12 hours, followed by calcination in a calcining furnace at 500°C for 5 hours. The solid was powdered in a mortar and pestle and stored in a sealed tube.

ii. Pd/Cerium oxide-alumina catalyst calcined at 850 °C

An aqueous solution was made by dissolving 0.388 g of palladium nitrate hydrate (Aldrich, USA) in 1.5 mL of distilled water in a 10 mL beaker. The 3.01 g solid cerium oxide-alumina dual support was calcined at 850 °C and added into the vortex tube with 5.0 mL of distilled water to make slurry. An aqueous precursor solution of palladium nitrate hydrate was added in 20 microliter increments to the aqueous solution of the dual support as it was being vortexed at speed 3 for 3 hrs. The slurry was dried in an air oven at 110°C for 12 hours, followed by calcination in a calcining furnace at 850°C for 5 hours. The solid was powdered in a mortar and pestle and stored in a sealed tube.

iii. Cerium oxide/Pd-alumina catalyst calcined at 500°C

2.14 g of palladium-alumina calcined at 500 °C was placed into a vortex tube along with 4 mL of distilled water and vortexed until a slurry formed. An aqueous solution was made by dissolving 0.951 g cerium nitrate hexahydrate in 1 mL of distilled water in a 10 mL beaker. An aqueous solution of cerium nitrate hexahydrate was added in 20 microliter increments to the aqueous solution of the dual support as it was being vortexed at speed 3 for 3 hrs. The slurry was dried in an air oven at 110°C for 12 hours, followed by calcination in a calcining furnace at 500°C for 5 hours. The solid was powdered in a mortar and pestle and stored in a sealed tube.

iv. Cerium oxide/Pd-alumina catalyst calcined at 850°C

2.13 g of palladium-alumina calcined at 850 °C was placed into vortex tube by adding 4 mL of distilled water and vortexing until a slurry formed. An aqueous solution was made by dissolving 0.959 g cerium nitrate hexahydrate in 1 mL of distilled water in a 10 mL beaker. An aqueous solution of cerium nitrate hexahydrate was added in 20 microliter increments to the aqueous solution of the dual support as it was being vortexed at speed 3 for 3 hrs. The slurry was

dried in an air oven at 110°C for 12 hours, followed by calcination in a calcining furnace at 850 °C for 5 hours. The solid was powdered in a mortar and pestle and stored in a sealed tube.

v. Dual support of cerium oxide/alumina calcined at 500°C and 850°C

3.034 g of cerium nitrate hexahydrate (Aldrich, USA) was dissolved in 2 mL of distilled water and taken in the sterile syringe. A slurry of solid 6.406 g γ -Al₂O₃ (Aldrich, USA) was made with 20 mL of distilled water in the vortex tube. The cerium nitrate solution was added in 20 microliter increments to the vortex tube while being vortexed at speed 3 and the solution was vortexed for 6 hours. The slurry was dried in an air oven at 110°C for 12 hours. The solid was powdered in a mortar and pestle and divided in half. Each half of the solids were calcined at 500°C and 850°C, respectively. After the calcination, it was stored in a sealed tube.

B. Catalytic Activity

The catalytic bed and the reactor unit are shown in Figures 4 and 5.



Figure 4. Catalyst bed in reactor

A mass of 0.10 g of a catalyst was packed in the reactor tube using quartz wool to hold the catalyst sample in place and quartz beads to allow the gas mixture to flow. Activity measurements were conducted in a temperature-controlled horizontal tubular fixed-bed quartz reactor (internal diameter 12mm) as shown in Figure 5. The catalyst bed was heated to a desired temperature using a temperature-controlled furnace (Carbolite MTF1000, Verder Scientific, Newtown, PA, USA). The reacting gas mixture consisted of 4% O₂, 1% CH₄ with the balance

nitrogen (NexAir, Memphis, TN, USA). The catalyst bed was heated to the desired temperature as nitrogen gas was being passed through the mass flow controller (Aalborg, Orangeburg, NY, USA). Each run ran the gas mixture through the quartz flow reactor tube for a length of 30 minutes at a fixed temperature and a flow of 150 cc/min. The catalyst bed was heated to a desired temperature as nitrogen gas was being passed using a temperature-controlled tube furnace. The temperature ranged from 250°C to 500°C.

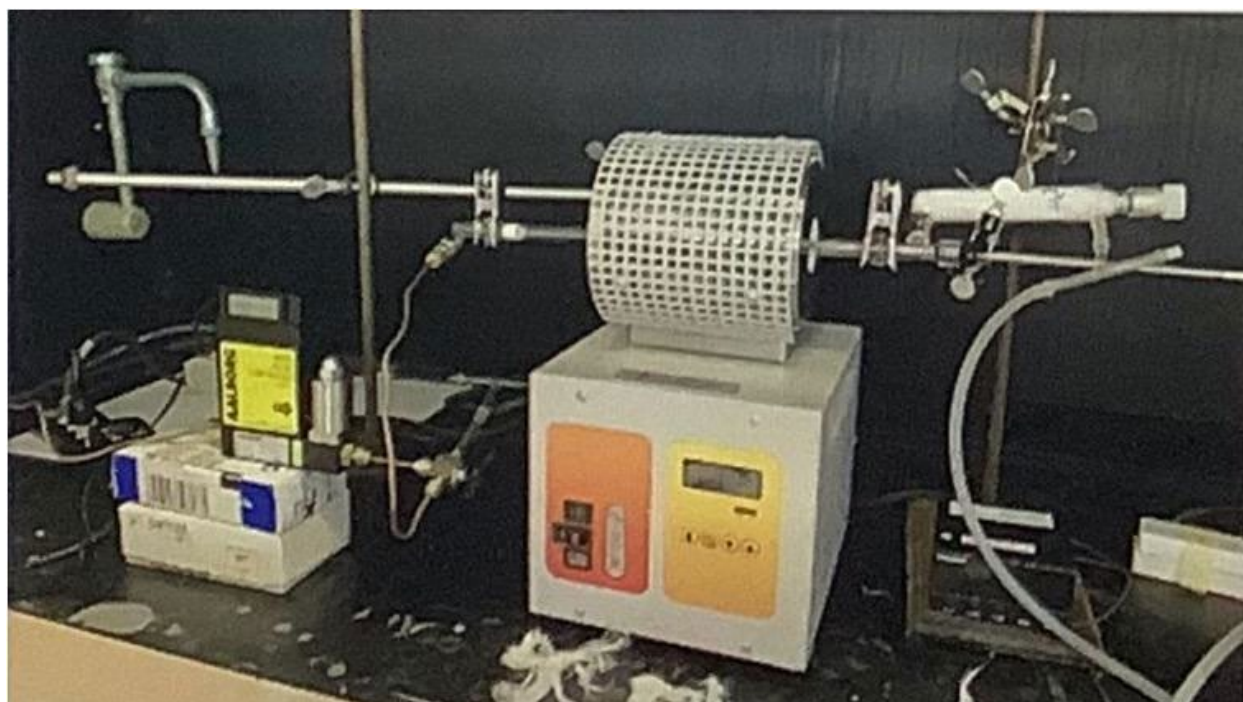


Figure 5. Catalytic reactor unit

Between each activity run, pure nitrogen gas was sent through the reactor tube to clear any leftover gas mixture. The reacted gas mixture was passed through a moisture trap to remove any moisture that may have occurred from the reaction. A volume of 1.0 cc of the outlet gas sample was collected in a gas tight syringe and injected to the column. The gas mixture was analyzed in a gas chromatography (HP 6850 series GC System, hp Hewlett Packard, USA) fitted

with a flame ionization detector, ‘Carbon Plot’ column, and ‘chemstation’ software. For all activity experiments, a gas flow rate of 150 cc/min (calculated at 25°C and 1 atm.), and a Gas Hourly Space Velocity (GHSV) of 90000 cc.g.cat-1.h-1 were chosen. The inlet and outlet gas feed composition were measured in volume % at 25°C and 1 atm.

For the activity experiment at each temperature, at least two runs were conducted. If the % conversions were within +/- 4% deviations between two consecutive runs, then the average of two runs at each temperature was used for the activity data. The conversion of methane ($v/v\%$) was calculated using the following equation:

$$\text{Conversion } (v/v\%) = \frac{[\text{CH}_4]_{\text{in}} - [\text{CH}_4]_{\text{out}}}{[\text{CH}_4]_{\text{in}}} \times 100\%$$

CH4 in = Volume% of methane at 1 atm. and 25 °C in the gas feed entering the reactor.

CH4 out = Volume% methane at 1 atm. and 25 °C in the gas mixture exiting the reactor.

C. Characterization

All characterizations except ICP-OES were conducted at the Georgia Institute of Technology as a part of a research collaboration.

i. Inductively Coupled Plasma Optical Emission Spectrometry (ICP-OES)

This analytical technique was used to determine the wt.% of Pd and Ce. The elemental analysis was conducted by Galbraith Laboratories, Inc. using Perkin Elmer 5300V (Akron, OH, USA). The sample was prepared by sodium peroxide fusion due to high % of Al₂O₃, followed by dissolution in water and acidification.

ii. Pulse Chemisorption

Pulse chemisorption experiments were conducted with both fresh and spent (after reaction with the methane gas mix) catalysts. Pd dispersion and metal particle size were measured with pulse chemisorption using CO as the probe gas. Approximately 50 mg of each

catalyst was heated in 20 mL/min of He (Airgas, PA, USA) at 200 °C for 2 hours to remove any water or other absorbed species. After that, the catalyst was cooled to 50 °C and temperature programmed reduction of the catalyst was performed using a flow of 10% H₂/He (20 mL/min). Temperature was increased to 450 °C at 5 °C/min and held for 1 hour. The sample was then cooled to 40 °C for the pulse CO testing. 20 doses of 10% CO/He (Airgas, PA, USA) were passed over the sample and adsorption peaks were analyzed using a thermal conductivity detector (TCD). Next, 20 mL/min of He flowed over the sample for 60 minutes to remove physisorbed species. A second round of 10% CO/He pulses was conducted to see if further CO could be adsorbed. Pulse CO chemisorption was performed in Micromeritics AutoChem II 2920 (Micromeritics Corporation, Norcross, GA, USA).²⁰

iii. Temperature-Programmed Reduction (TPR)

Approximately 50 mg of each catalyst was heated in 20 mL/min of He (UHP, Airgas, PA, USA) to 200 °C at 5 °C/min, held 2 hours, and then cooled to 50 °C in a 20 mL/min flow of 10% H₂/He. The catalyst was then reduced by increasing the temperature to 800 °C at a ramp rate of 5 °C/min under a flow of 10% H₂/He (20 mL/min). The effluent gas flow was fed through a cold trap of liquid nitrogen and acetone and then into a thermal conductivity detector (TCD) to find hydrogen uptake. Temperature programmed reduction with hydrogen (TPR) and was performed in Micromeritics AutoChem II 2920 (Micromeritics Corporation, Norcross, GA, USA).

iv. X-Ray Photoelectron Spectroscopy (XPS)

Ex-situ X-ray photoelectron spectroscopy (XPS) analysis was conducted with both fresh and spent (after reaction with the methane gas mix) catalysts. XPS was performed with a Thermo K-Alpha spectrometer (ThermoFisher Scientific, Waltham, MA, USA), using a monochromatic Al K α radiation source. Spectra were measured in the regions of Pd3d, O1s, and Ce3d. Charge

referencing was performed from the C1s region, referenced to the adventitious carbon (at 284.8 eV). The X-ray beam spot size was a 400 μm and the spectrometer was run at 50 eV pass energy and 50 ms dwell time for each step size of 0.1 eV. The deconvolutions of the Pd3d and Ce3d peaks were performed by *Avantage* software.

v. High-Angle Annular Dark-Field Scanning Transmission Electron Microscopy (HAADF-STEM)

This characterization is used to find the morphology and location of PdO and CeOx particles on ceria/alumina supports. A Hitachi HD2700 (Hitachi Ltd., Tokyo, Japan) aberration-corrected scanning transmission electron microscope was used to record HAADF-STEM images. The samples were prepared on a lacey carbon-coated Au grid.²¹

III. RESULTS AND DISCUSSION

A. Activity of the Catalysts

The activity data is given in Table 2.

Table 2. Activity data on methane combustion at 500 °C and 850 °C with fresh catalysts

Catalyst	% Methane conversion	
	Reaction at 500 °C	Reaction at 850°C
Pd/cerium oxides-alumina 500C	100	-
Pd/cerium oxides-alumina 850C	80	100
Cerium oxides/Pd-alumina 500C	86	-
Cerium oxides/Pd-alumina 850C	68	93
Cerium oxides/alumina 500C	18	-
Cerium oxides/alumina 850C	20	98

Conditions: particle size -200+270 ASTM sieve; Steady state with GHSV, 90000(cc/cc)/ g.cat/ hr and reaction time, 60 min.

Table 2 compares the activities of the catalysts and the dual support at 500 °C and 850 °C. The activities of Pd/cerium oxides-alumina catalysts were higher than those of cerium oxides/Pd-alumina catalysts at 500 °C. However, the activities of Pd/cerium oxides-alumina 850C catalyst and the cerium oxides/Pd-alumina 850C catalyst were similar indicating that the effect of impregnation sequence was more perceptible at lower reaction temperatures.

Table 3 and Figure 6 show activities of Pd/cerium-alumina oxides catalysts were much higher compared to Ce oxides/Pd-alumina catalyst at both calcination temperatures of 500 °C and 850 °C. Both catalysts showed higher activities at 500 °C compared to 850 °C. The results show the sequence of impregnation and calcination temperature has immense effects on activity. The results also show each catalyst had different light-off temperatures. Better activity of Pd/CeO₂/Al₂O₃ catalysts has also been reported by earlier researchers.^{12,17,18,22}

Tables 2 and 4 display the activities of the cerium oxides-aluminum oxide dual support calcined at 500 °C and 850 °C. The activity of the dual support cerium oxides/alumina500C was low (below 20%) at a reaction temperature of 500 °C. We found an interesting result with the cerium oxides/alumina850C dual support . It showed high activities (82-94%) at 800 °C-850 °C without impregnating the palladium catalyst. The cerium oxidation states play a significant role in the catalytic process which needs further research on the dual support.

Table 3. Activity-Temperature data

Reaction Temp, 0 °C	Methane Conversion			
	Pd/cerium oxides- alumina 500C	Cerium oxides/Pd- alumina500C	Pd/cerium oxides- alumina850C	Cerium oxides/Pd- alumina850C
250	5.5	3.6	5.0	0
275	17.0	12.3	7.8	5.3
300	27.9	18.4	14.5	6.9
325	55.0	21.0	29.7	9.0
350	74.1	37.2	60.0	9.2
375	84.5	46.4	64.7	13.8
400	87.8	58.5	68.7	16.0
450	93.7	74.7	82.9	20.8
500	98.2	85.0	92.9	33.1
550	-	-	-	64.1
600	-	-	-	80.5
850	-	-	100	100

Conditions: particle size -200+270 ASTM sieve; Steady state with GHSV, 90000(cc/cc)/ g.cat/ hr and reaction time, 30min.

Table 4. Activity data of Cerium oxides/alumina 850C

Temperature	% Conversion
300	9.5
400	12.3
500	16
600	17.7
700	34.9
800	82.1
850	93.7

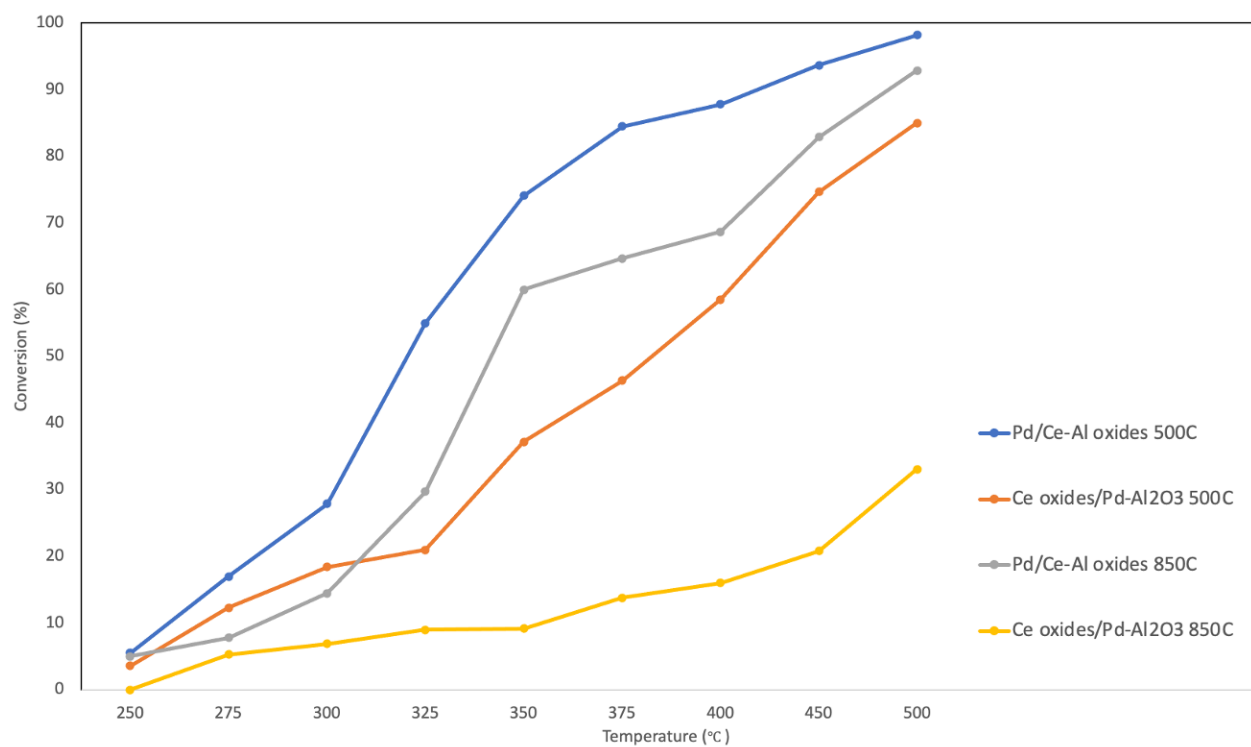


Figure 6. Methane conversion at different temperatures

[GHSV, 90,000 (cc/g.cat) h⁻¹; reaction time at each temperature, 30 min; inlet gas mix composition, 0.98% CH₄, 4.0 % O₂, balance N₂]

i.i. Activation energy

Table 5 gives the activity data for the determination of activation energy of the four catalysts. Figure 7 shows the Arrhenius plots for the four catalytic reactions. The kinetic regions of temperatures with methane conversions below 30% were used for calculating the activation energies. The activation energies of Pd/cerium oxides-alumina500C and Pd/cerium oxides-alumina850C were 110.8 kJ/mol and 152.8 kJ/mol, respectively. Similarly, the activation energies of cerium oxides/Pd-alumina500C and cerium oxides/Pd-alumina850C catalysts were 113.6 kJ/mol and 195 kJ/mol, respectively. The lower activation energies of methane combustion for the Pd/cerium oxides-alumina 500C and 850C catalysts explain the higher activities of these catalysts compared to the cerium oxides/Pd-alumina 500C and 850C catalysts.

Table 5. Activation energy

Temperature (°C)	Conversion (%)			
	Pd/cerium oxides-alumina500C	Cerium oxides/Pd-alumina500C	Pd/cerium oxides-alumina850C	Cerium oxides/Pd-alumina850C
250	5.5	3.6		
260	12.0			
265		5.9		
270	14.0			
275		12.3		
310			8.0	
315			21.7	
325			29.7	
440				10.6
450				24.8
460				25.9
Ea, kJ/mol	110.8	113.6	152.8	195.0

Conditions: particle size -200+270 ASTM sieve, Steady state with GHSV, 90000 (cc/cc)/g.cat/hr and reaction time, 30 min.

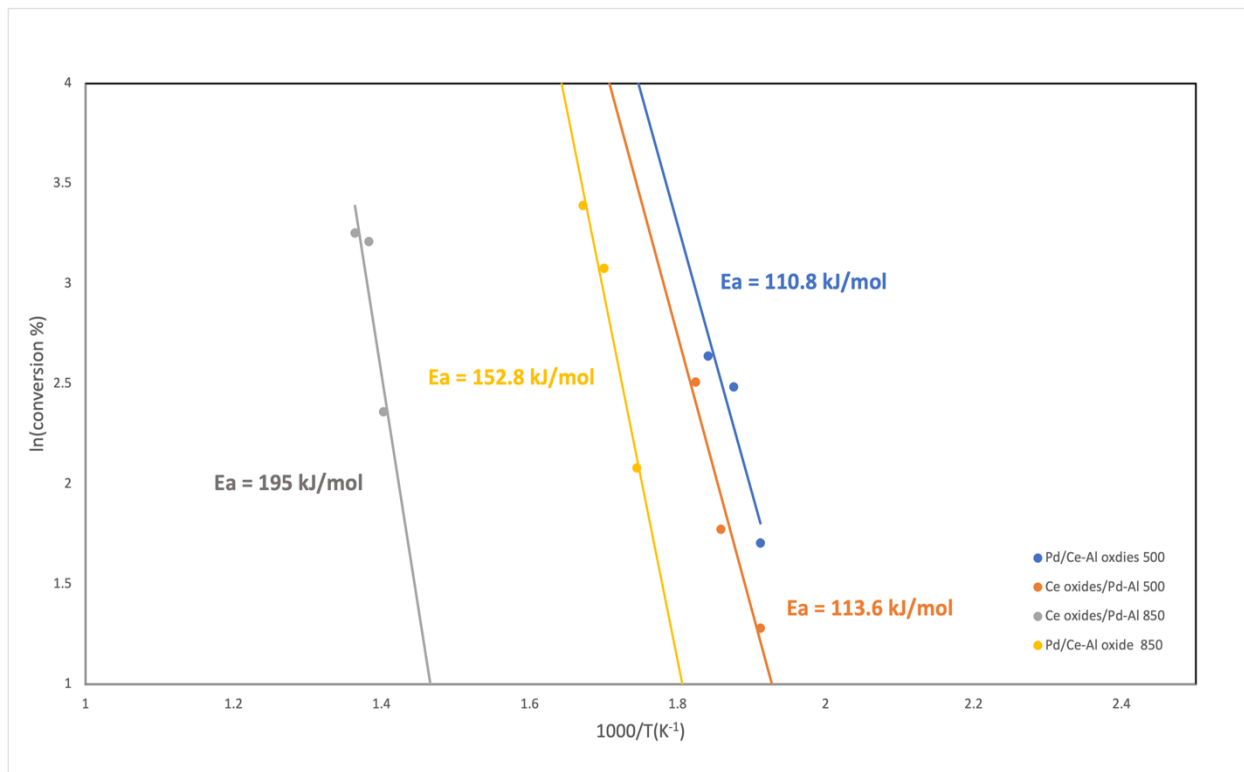


Figure 7. Activation energy for methane combustion with the four catalysts

i.ii. Stability test

Table 6 gives the data for the stability test of the four catalysts. The stability tests were conducted for each catalyst at temperatures corresponding to about 30% conversion. Table 6 reports the activity for each catalyst after 60 min and 24 hours of reaction with the reacting gas mixture of 1% methane, 4% oxygen and balance nitrogen. Stability test decides if a catalyst is still stable and active after 24 hours. The decrease of about 4% in conversion for the cerium oxides/Pd-alumina500C catalyst after 24 hours was within the range of experimental errors as mentioned in the methods section. The stability of the cerium oxides/Pd-alumina500C catalyst was better than the Pd/cerium oxides-alumina 500C catalyst. The Pd/cerium oxides-alumina and cerium oxides/Pd-alumina catalysts calcined at 850 °C showed similar stability.

Table 6. Stability test on four catalysts

Catalyst	Methane Conversion, %		
	1hr	24hrs	Temperature
Pd/cerium oxides-alumina 500C	29.5	17.7	285 °C
Pd/cerium oxides-alumina 850C	22.7	22.4	325 °C
Cerium oxides/Pd-alumina 500C	31.8	27.0	350 °C
Cerium oxides/Pd-alumina 850C	32.0	31.5	480 °C

The results on activity of the catalysts could be summarized as follows:

Pd/cerium oxides-alumina 500C is the best catalyst (Table 3) at a lower temperature range of 350-375 °C, and both Pd/cerium oxides-alumina 500C and 850C catalysts have high activity (90%) at 500 °C. Cerium oxides/Pd-alumina 500C and 850C catalysts had much lower activities at and below 400 °C. The results support earlier research showing sequence of impregnation had high influence on catalytic activity.¹⁹ The activation energies of the four catalysts also explain the difference in the activities.

B. Characterization

ii.i. Inductively Coupled Plasma Optical Emission Spectrometry (ICP-OES)

The palladium and ceria contents were analyzed by ICP-OES method. The data in Table 7 show the calculated and experimental % of Pd and Ce in the catalyst were similar within the range of experimental error.

Table 7. % Pd and Ce in Pd/Ceria-alumina 850C catalyst

	Calculated	ICP-OES
% Pd	4.0%	4.7%
% Ce	12.2%	10.6%

ii.ii. Pulse Chemisorption

Both fresh and spent Pd/cerium oxides-alumina catalysts have higher dispersion and smaller nanoparticle diameter compared to cerium oxides/Pd-alumina catalysts at two calcination temperatures of 500 °C and 850 °C. The dispersion of Pd/cerium oxides-alumina500C catalyst was much higher compared to the cerium oxides/Pd-alumina catalyst500C catalyst. The higher dispersion and the lower particle size explain why the Pd/cerium oxides-alumina500C had much higher activity compared to the cerium oxides/Pd-alumina catalyst500C catalyst. However, the dispersion effects were not so perceptible between the two catalysts at 850 °C calcination temperature. As reported in Table 8, both dispersion and particle size of the four catalysts showed big differences. The results are similar with the work of Sun et al.¹⁵ and Onn et al.²³

Table 8 . Properties of catalysts

Properties	Pd/cerium oxides-alumina500C	Pd/cerium oxides-alumina850C	Cerium oxides/Pd-alumina500C	Cerium oxides/Pd-alumina850C
Dispersion (%)	37.7	6.5	7.3	4.4
Nanoparticle diameter (hemisphere) (nm)	3.0	17.1	15.3	25.2

ii.iii. Hydrogen-Temperature Programmed Reduction (H₂-TPR)

The H₂-TPR results are shown in Figure 8. The peaks at 195-215 °C are due to reduction of relatively large PdO/PdOx particles under weak interaction with the support and or desorption of H₂ adsorbed by Pd/PdO.¹⁷ The stronger reduction peak at 220-256 °C and 327-417 °C could be due to reduction of PdO/PdOx particles under strong interaction with the support.¹⁴ The peak intensities in these temperature ranges are much higher for Pd/cerium oxides-alumina 500C and 850C catalysts compared to the cerium oxides/Pd-alumina 500C and 850C catalysts indicating stronger metal-support interactions in Pd/cerium oxides-alumina catalysts (Pd impregnated on ceria-alumina supports).

The TPR results explain the methane activities (Table 3) at low temperatures; the cerium oxides/Pd-alumina 500C and 850C catalysts showed lower activities at 250-375 °C since the active phases of PdO/PdOx particles were loosely adsorbed on the alumina-ceria support in this temperature range due to the weaker metal-support interactions. The peak at 430-477 °C could be due to reduction of bulk CeO₂.¹⁸ The reduction of peak intensities in Pd/cerium oxides-alumina 850C and cerium oxides/Pd-alumina 850C are much lower showing weaker interaction of ceria in the dual support and the higher calcination temperature had effects in the ceria chemistry. The high-temperature reduction peaks at 785-790 °C are weak in intensities and suggest reduction of ceria strongly held on the surface.

In heterogeneous catalytic reactions, factors including particle size, chemical composition, and metal-support interactions could have a noticeable influence on the catalytic properties of metal catalysts.²⁴

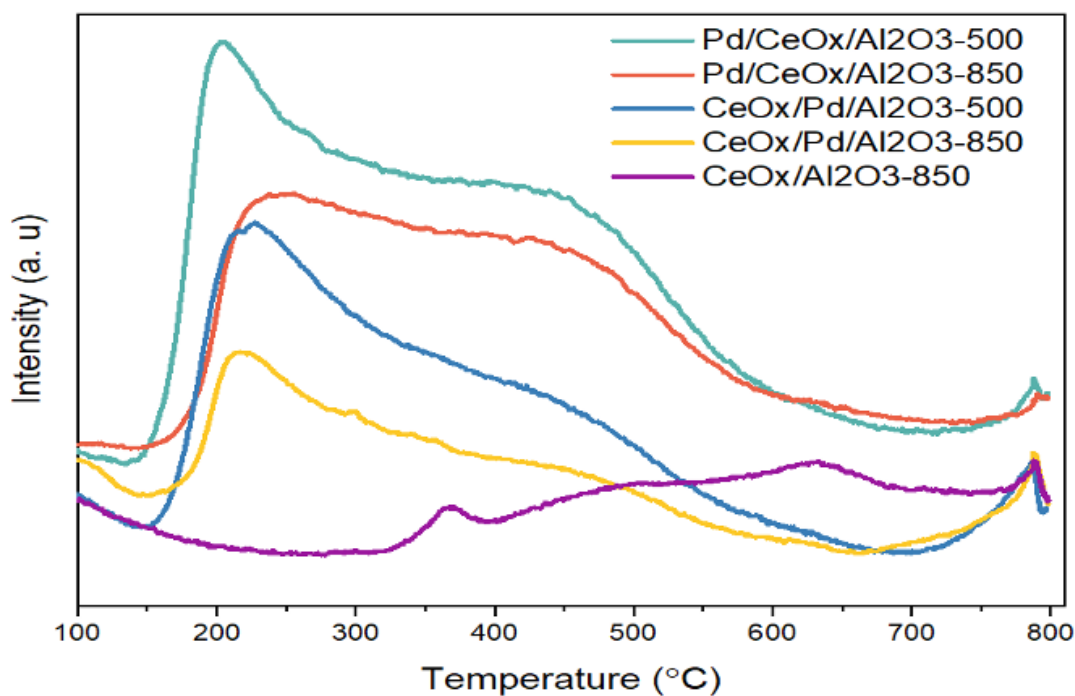


Figure 8. Hydrogen-TPR

ii.iv. X-Ray Photoelectron Spectroscopy (XPS)

XPS measures the oxidation states of palladium and Ce and the atomic % of the Pd element/compounds in different oxidation states. The data on XPS is given in Table 9. All catalysts had palladium as PdO and PdO_x x>2+, with tiny amounts of Pd⁰; PdO_x x>2+ denotes nonstoichiometric PdO. The trends in the variation of at% of the Pd species before and after are not clear. %. The only noticeable difference was a higher % of PdO in the Ce oxides/Pd- alumina catalysts compared to the Pd/ceria-alumina catalysts. All fresh and spent catalysts had varying amounts of Ce (II) and Ce (IV) oxides. The Pd/cerium oxides-alumina500C catalyst had 70 at% of Ce(IV) and 30 at% of Ce(III) while the cerium oxides/Pd- alumina500C catalyst had 54 at% Ce(IV) and 46 at% Ce(III). It appears the higher methane activity of the Pd/cerium oxides-alumina500C catalyst was related to the Ce(IV) %. Another interesting feature was the presence of both Ce(IV) and

Ce(III) in the dual support of cerium oxides-alumina calcined at 500 °C and 850 °C. The precursor for the cerium oxide was Ce (III) nitrate. The fresh catalysts were calcined at 500 °C and 850 °C for 5 hours, but still had Ce (III). Ce is supposed to be in Ce (IV) state after calcination at these elevated temperatures. It is not clear why Ce (III) was present in the fresh catalysts. It appears interactions and interplay between Ce and Pd oxidation states play a role in the catalytic oxidation process. One possibility could be oxidation of Pd⁰ to Pd⁺² and reduction of Ce⁺⁴ to Ce⁺³ during the calcination process.

Table 9. Atomic % of Pd, PdO and PdO_x based on deconvolutions of 3d5/2 peak in the Pd 3dXPS spectra

Catalysts /Supports	Pd, at%	PdO, at%	PdO _{x, x>2+} , at%
Pd/cerium oxides-alumina500C	6	58	36
Pd/cerium oxides-alumina850C	5	59	36
Cerium oxides/Pd-alumina500C	0	65	35
Cerium oxides/Pd-alumina850C	0	87	13

ii.v. High-Angle Annular Dark-Field Scanning Transmission Electron Microscopy (HAADF-STEM) and Scanning Electron Microscopy (SEM)

The HAADF-STEM images of the four catalysts are shown in Figure 9. In Figure 9 (a), the red arrows show small PdO particles on alumina and CeOx (designating cerium oxides) and the blue arrows show large cluster of CeOx particles on alumina; the frame in Figure 9(b) shows small PdOx particles mostly on CeOx and large CeOx particles on alumina; frame (c) indicates that the PdO particles are embedded on CeOx ; frame (d) also shows PdO particles are embedded on CeOx and the structures are distorted when the catalyst was heated to 850 °C. The STEM images of cerium oxides/Pd-alumina500C catalyst show different morphology and distribution of

PdOx particles on CeOx and alumina support compared to the images of Pd/cerium oxides-alumina500C catalyst. The smaller particles sizes mostly on the surface of alumina account for the higher activity of Pd/cerium oxides-alumina 500C catalyst. It appears an elevated temperature calcination of the catalyst made the PdOx particles engraved on CeOx due to agglomeration, and this had effect of lowering the activity of this catalyst. Huang et al.²⁵ studied the activities of Pd/CeO₂-Al₂O₃ catalysts in different calcination temperature and saw both metallic Pd and PdO are the active sites for methane oxidation while PdO had a vital role. Also, smaller Pd particles improved the methane combustion due to stronger Pd-Ce interaction.

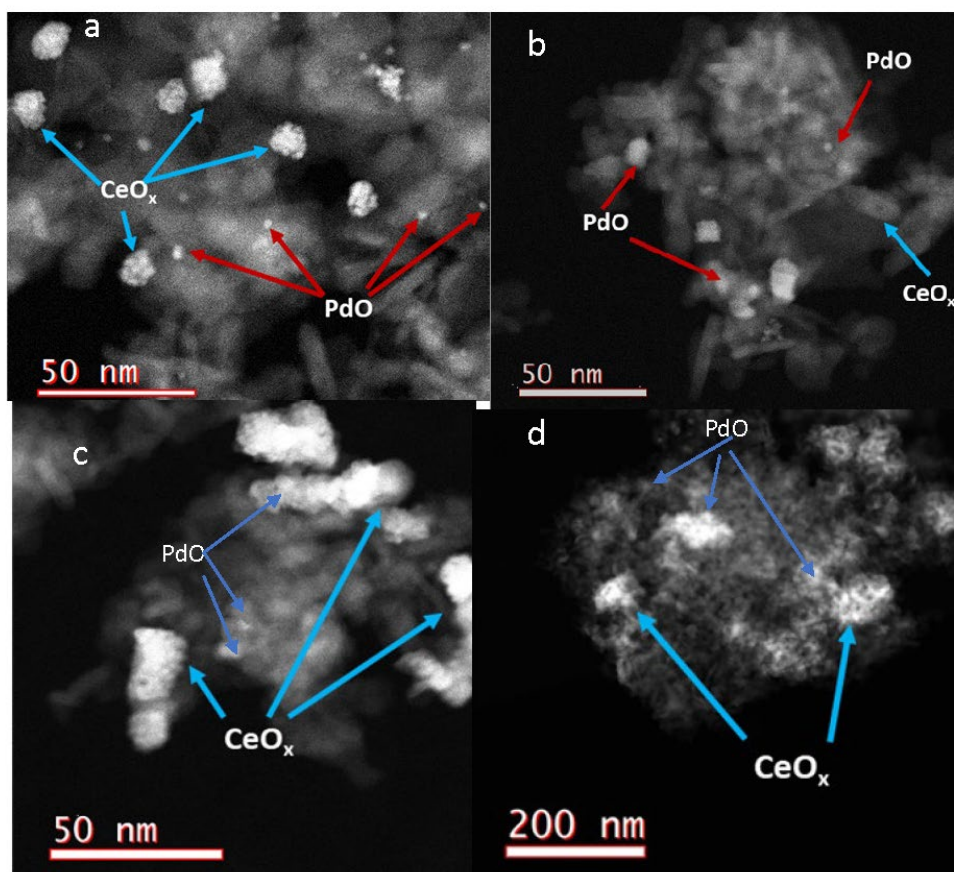


Figure 9. STEM images of four catalysts. (a) STEM image of Pd/cerium oxides-alumina500C; (b) Pd/cerium oxides-alumina850C; (c) Cerium oxides/Pd-alumina500C; (d) Cerium oxides/Pd-alumina850C

IV. CONCLUSION

Four catalysts were synthesized by changing the sequence of impregnation of palladium and cerium oxides, and the calcination temperature. All four catalysts had 4.7 wt.% Pd as PdO and PdO_x (x>2+), 10.7 wt.% cerium as CeO_x (in +3 and +4 oxidation states) and balance γ -Al₂O₃ based on ICP-OES analysis. The activities for methane oxidation of the Pd/cerium oxides-alumina oxide catalysts calcined at 500 °C and 850 °C were higher below 500 °C compared to the cerium oxides/Pd-alumina catalysts under the same conditions. STEM imaging and pulse chemisorption data supplied the main supporting evidence. The higher dispersion and smaller particles sizes account for the higher activity of the Pd/cerium oxides-alumina 500C catalyst. The TPR showed that Pd/cerium oxides-alumina catalysts have stronger metal-support interaction which supports the methane activities at low temperatures. Ce oxides/Pd- Al₂O₃ catalysts showed lower activities since the active phases of PdO/PdO_x particles were embedded on the ceria support due to agglomeration. The catalysts calcined at 850 °C may have weaker interaction of ceria so the high calcination temperature might contribute to the ceria chemistry. The STEM image of Pd/cerium oxides-alumina catalyst calcined at 500 °C showed small PdO particles on the surface of alumina and cerium oxides. In the cerium oxides/Pd-alumina catalyst calcined at 500 °C, only a small number of PdO particles were on both CeO_x and alumina, and the majority of PdO_x particles were engraved on the CeO_x support. This accounted for the lower activities of this catalyst.

The support alumina could ease oxygen mobility and from the bulk in the Pd/CeO₂-Al₂O₃ could stabilize the PdO particles.²⁶⁻²⁷ Nilsson et al.²⁸ reported the chemical state of alumina- and ceria- supported palladium nanoparticles and found the high catalytic activities were due to the

presence of reduced Pd or PdOx sites. The reducibility of an oxide by metal nanoparticles in metal/oxide interaction could change the catalytic activity.²⁹

V. BIBLIOGRAPHY

- (1) Methane: A crucial opportunity in the climate fight | Environmental Defense Fund <https://www.edf.org/climate/methane-crucial-opportunity-climate-fight> (accessed 2022 -03 -17).
- (2) Overview of Greenhouse Gases | US EPA <https://www.epa.gov/ghgemissions/overview-greenhouse-gases> (accessed 2022 -03 -17).
- (3) Jiang, D.; Khivantsev, K.; Wang, Y. Low-Temperature Methane Oxidation for Efficient Emission Control in Natural Gas Vehicles: Pd and Beyond. *ACS Catalysis* **2020**, *10* (23), 14304–14314. <https://doi.org/10.1021/acscatal.0c03338>.
- (4) Monai, M.; Montini, T.; Gorte, R. J.; Fornasiero, P. Catalytic Oxidation of Methane: Pd and Beyond. *European Journal of Inorganic Chemistry*. Wiley-VCH Verlag July 6, 2018, pp 2884–2893. <https://doi.org/10.1002/ejic.201800326>.
- (5) Chen, J.; Arandiyán, H.; Gao, X.; Li, J. Recent Advances in Catalysts for Methane Combustion. *Catalysis Surveys from Asia*. Springer New York LLC September 1, 2015, pp 140–171. <https://doi.org/10.1007/s10563-015-9191-5>.
- (6) Simplicio, L. M. T.; Brandão, S. T.; Sales, E. A.; Lietti, L.; Bozon-Verduraz, F. Methane Combustion over PdO-Alumina Catalysts: The Effect of Palladium Precursors. *Applied Catalysis B: Environmental* **2006**, *63* (1–2), 9–14. <https://doi.org/10.1016/j.apcatb.2005.08.009>.
- (7) Goodman, E. D.; Dai, S.; Yang, A. C.; Wrasman, C. J.; Gallo, A.; Bare, S. R.; Hoffman, A. S.; Jaramillo, T. F.; Graham, G. W.; Pan, X.; Cargnello, M. Uniform Pt/Pd Bimetallic Nanocrystals Demonstrate Platinum Effect on Palladium Methane Combustion Activity and Stability. *ACS Catalysis* **2017**, *7* (7), 4372–4380. <https://doi.org/10.1021/acscatal.7b00393>.
- (8) Banerjee, A. C.; McGuire, J. M.; Lawnick, O.; Bozack, M. J. Low-Temperature Activity and PdO-PdOx Transition in Methane Combustion by a PdO-PdOx/ γ -Al₂O₃ Catalyst. *Catalysts* **2018**, *8* (7). <https://doi.org/10.3390/catal8070266>.
- (9) Colussi, S.; Trovarelli, A.; Cristiani, C.; Lietti, L.; Groppi, G. The Influence of Ceria and Other Rare Earth Promoters on Palladium-Based Methane Combustion Catalysts. *Catalysis Today* **2012**, *180* (1), 124–130. <https://doi.org/10.1016/j.cattod.2011.03.021>.
- (10) Ma, J.; Lou, Y.; Cai, Y.; Zhao, Z.; Wang, L.; Zhan, W.; Guo, Y.; Guo, Y. The Relationship between the Chemical State of Pd Species and the Catalytic Activity for Methane Combustion on Pd/CeO₂. *Catalysis Science and Technology* **2018**, *8* (10), 2567–2577. <https://doi.org/10.1039/c8cy00208h>.
- (11) Cargnello, M.; Delgado Jaén, J. J.; Garrido, J. C. H.; Bakhmutsky, K.; Montini, T.; Calvino Gámez, J. J.; Gorte, R. J.; Fornasiero, P. *Exceptional Activity for Methane Combustion over Modular Pd@CeO₂ Subunits on Functionalized Al₂O₃*.
- (12) Li, L.; Zhang, N.; Wu, R.; Song, L.; Zhang, G.; He, H. Comparative Study of Moisture-Treated Pd@CeO₂/Al₂O₃ and Pd/CeO₂/Al₂O₃ Catalysts for Automobile Exhaust Emission Reactions: Effect of Core-Shell Interface. *ACS Applied Materials and Interfaces* **2020**, *12* (9), 10350–10358. <https://doi.org/10.1021/acsami.9b20734>.

- (13) Rodrigues, L. M. T. S.; Silva, R. B.; Rocha, M. G. C.; Bargiela, P.; Noronha, F. B.; Brandão, S. T. Partial Oxidation of Methane on Ni and Pd Catalysts: Influence of Active Phase and CeO₂ Modification. *Catalysis Today* **2012**, *197* (1), 137–143. <https://doi.org/10.1016/j.cattod.2012.07.031>.
- (14) Ramírez-López, R.; Elizalde-Martinez, I.; Balderas-Tapia, L. Complete Catalytic Oxidation of Methane over Pd/CeO₂-Al₂O₃: The Influence of Different Ceria Loading. *Catalysis Today* **2010**, *150* (3–4), 358–362. <https://doi.org/10.1016/j.cattod.2009.10.007>.
- (15) Sun, M.; Hu, W.; Yuan, S.; Zhang, H.; Cheng, T.; Wang, J.; Chen, Y. Effect of the Loading Sequence of CeO₂ and Pd over Al₂O₃ on the Catalytic Performance of Pd-Only Close-Coupled Catalysts. *Molecular Catalysis* **2020**, *482*. <https://doi.org/10.1016/j.mcat.2017.10.002>.
- (16) Colussi, S.; Trovarelli, A.; Vesselli, E.; Baraldi, A.; Comelli, G.; Groppi, G.; Llorca, J. Structure and Morphology of Pd/Al₂O₃ and Pd/CeO₂/Al₂O₃ Combustion Catalysts in Pd-PdO Transformation Hysteresis. *Applied Catalysis A: General* **2010**, *390* (1–2), 1–10. <https://doi.org/10.1016/j.apcata.2010.09.033>.
- (17) Liu, X.; Liu, J.; Geng, F.; Li, Z.; Li, P.; Gong, W. Synthesis and Properties of PdO/CeO₂-Al₂O₃ Catalysts for Methane Combustion. *Frontiers of Chemical Science and Engineering* **2012**, *6* (1), 34–37. <https://doi.org/10.1007/s11705-011-1163-3>.
- (18) Yang, X.; Du, C.; Guo, Y.; Guo, Y.; Wang, L.; Wang, Y.; Zhan, W. Al₂O₃ Supported Hybrid Pd–CeO₂ Colloidal Spheres and Its Enhanced Catalytic Performances for Methane Combustion. *Journal of Rare Earths* **2019**, *37* (7), 714–719. <https://doi.org/10.1016/j.jre.2018.10.005>.
- (19) Fertal, D. R.; Bukhovko, M. P.; Ding, Y.; Billor, M. Z.; Banerjee, A. C. Particle Size and PdO–Support Interactions in PdO/CeO₂- γ -Al₂O₃ Catalysts and Effect on Methane Combustion. *Catalysts* **2020**, *10* (9), 1–16. <https://doi.org/10.3390/catal10090976>.
- (20) Sulmonetti, T. P.; Pang, S. H.; Claire, M. T.; Lee, S.; Cullen, D. A.; Agrawal, P. K.; Jones, C. W. Vapor Phase Hydrogenation of Furfural over Nickel Mixed Metal Oxide Catalysts Derived from Layered Double Hydroxides. *Applied Catalysis A: General* **2016**, *517*, 187–195. <https://doi.org/10.1016/j.apcata.2016.03.005>.
- (21) Ding, Y.; Chen, Y.; Pradel, K. C.; Zhang, W.; Liu, M.; Wang, Z. L. Domain Structures and Prco Antisite Point Defects in Double-Perovskite PrBaCo₂O_{5+ δ} and PrBa_{0.8}Ca_{0.2}Co₂O_{5+ δ} . *Ultramicroscopy* **2018**, *193*, 64–70. <https://doi.org/10.1016/j.ultramic.2018.06.008>.
- (22) Feng, X.; Li, W.; Liu, D.; Zhang, Z.; Duan, Y.; Zhang, Y. Self-Assembled Pd@CeO₂/ γ -Al₂O₃ Catalysts with Enhanced Activity for Catalytic Methane Combustion. *Small* **2017**, *13* (31). <https://doi.org/10.1002/smll.201700941>.
- (23) Onn, T. M.; Zhang, S.; Arroyo-Ramirez, L.; Xia, Y.; Wang, C.; Pan, X.; Graham, G. W.; Gorte, R. J. High-Surface-Area Ceria Prepared by ALD on Al₂O₃ Support. *Applied Catalysis B: Environmental* **2017**, *201*, 430–437. <https://doi.org/10.1016/j.apcatb.2016.08.054>.
- (24) Liu, L.; Corma, A. Metal Catalysts for Heterogeneous Catalysis: From Single Atoms to Nanoclusters and Nanoparticles. *Chemical Reviews*. American Chemical

- Society May 23, 2018, pp 4981–5079.
<https://doi.org/10.1021/acs.chemrev.7b00776>.
- (25) Huang, F.; Chen, J.; Hu, W.; Li, G.; Wu, Y.; Yuan, S.; Zhong, L.; Chen, Y. Pd or PdO: Catalytic Active Site of Methane Oxidation Operated Close to Stoichiometric Air-to-Fuel for Natural Gas Vehicles. *Applied Catalysis B: Environmental* **2017**, *219*, 73–81. <https://doi.org/10.1016/j.apcatb.2017.07.037>.
- (26) Miller, J. B.; Malatpure, M. Pd Catalysts for Total Oxidation of Methane: Support Effects. *Applied Catalysis A: General* **2015**, *495*, 54–62.
<https://doi.org/10.1016/j.apcata.2015.01.044>.
- (27) Schwartz, W. R.; Pfefferle, L. D. Combustion of Methane over Palladium-Based Catalysts: Support Interactions. *Journal of Physical Chemistry C* **2012**, *116* (15), 8571–8578. <https://doi.org/10.1021/jp2119668>.
- (28) Nilsson, J.; Carlsson, P. A.; Fouladvand, S.; Martin, N. M.; Gustafson, J.; Newton, M. A.; Lundgren, E.; Grönbeck, H.; Skoglundh, M. Chemistry of Supported Palladium Nanoparticles during Methane Oxidation. *ACS Catalysis* **2015**, *5* (4), 2481–2489. <https://doi.org/10.1021/cs502036d>.
- (29) Puigdollers, A. R.; Schlexer, P.; Tosoni, S.; Pacchioni, G. Increasing Oxide Reducibility: The Role of Metal/Oxide Interfaces in the Formation of Oxygen Vacancies. *ACS Catalysis*. American Chemical Society October 6, 2017, pp 6493–6513. <https://doi.org/10.1021/acscatal.7b01913>.

SYNTHESIS, CHARACTERIZATION AND ACTIVITY OF PALLADIUM CATALYSTS ON
THE DUAL SUPPORT OF CERIUM AND ALUMINUM OXIDES

A thesis submitted to the College of Letters and Science in partial fulfillment of the
requirements for the degree of

MASTER OF SCIENCE

DEPARTMENT OF CHEMISTRY

by

Jihyeon park

2022

Dr. Anil C. Banerjee

Date

Dr. Zewdu Gebeyehu

Date

Dr. D. Wade Holley

Date